Electronic Supplementary Material (ESI) for Nanoscale.

Movable type printing method to fabricate ternary FeCoNi alloy confined in porous carbon towards oxygen electrocatalysts for rechargeable Zn-air battery

Xuzi Cong[a,1], Jigang Wang[a,1], Yinggang Sun[a], Gaojin Feng[a], Qiang Liu[a], Likai Wang[a,b,*]

[a] School of Chemistry and Chemical Engineering, Shandong University of Technology, Zibo, Shandong 255049, P. R. China

[b] School of Chemical and Biological Engineering, and Institute of Chemical Process, Seoul National University, Seoul 08826, Republic of Korea.

* Corresponding authors.

E-mail addresses: lkwangchem@sdut.edu.cn

[1] These authors contributed equally to this work.

Electrochemical Characterizations

The electrochemical measurements were conducted using CHI 760E electrochemical workstation equipped with a standard three-electrode glass cell. The three-electrode consisted of a reference electrode (Ag/AgCl), a counter electrode (graphite rod) and a rotating disk electrode (RDE). For preparation of the working electrode, 2.5 mg of catalyst and 10 μL of Nafion (5 wt%) were dispersed in 1 mL ethanol under sonication for 30 mins to obtain a uniform catalyst ink. Subsequently, 32 μL of the catalyst ink was carefully applied onto the surface of was dripped on the surface of RDE with the loading mass of 400 μg cm^{-2}, while the loading mass of commercial Pt/C was about 200 μg cm^{-2}.

The Koutecky-Levich (K-L) plot was calculated to obtain the number of electrons transferred (n) of oxygen reduction reaction and analyze reaction kinetic, could be expressed as follows:

$$\frac{1}{J}=\frac{1}{J_L}+\frac{1}{J_k}=\frac{1}{B\omega^{1/2}}+\frac{1}{J_K}$$

$$B=0.62nFC_0D_0^{2/3}\upsilon^{-1/6}$$

$$J_K=nFKC_0$$

where J, J_K and J_L are the measured current density, kinetic and diffusion limiting current densities, respectively; ωis the linear rotation speed (rpm min^{-1}) of the disk, F is the Faradaic constant (96485 C mol^{-1}), C_0 is the oxygen concentration (solubility) in 0.1 M KOH (1.2×10^{-6} mol cm^{-1}); D_0 is the oxygen diffusion coefficient in 0.1 M KOH (1.9×10^{-5} cm^2 s^{-1}), υ is the kinematic viscosity of the 0.1 M KOH (1.13×10^{-5} cm^2 s^{-1}), and K is the constant of electron transfer rate.

RRDE tests were conducted on the CHI 760E electrochemical analyzer at a rotation speed of 1600 rpm with a potential sweep of 10 mV s^{-1}; the Pt ring potential was set at 1.5 V vs. RHE. The electron transfer number (n) and the yield of hydrogen peroxide were obtained based on the following equation:

$$n = 4\frac{I_d}{I_d + I_r/N}$$

$$H_2O_2\% = 200\frac{I_r/N}{I_d + I_r/N}$$

where I_d and Ir are the disk current and ring current, respectively, and N is the collection efficiency of the Pt ring (N = 0.37, as provided by the manufacturer).

Liquid ZABs

Liquid ZABs were prepared and tested at room temperature. Briefly, a polished zinc foil and 6.0 M KOH filled with 0.2 M $Zn(acac)_2$ were used as anode and electrolyte, respectively. The air cathode was assembled with the carbon cloth loaded with FeCoNi-NC catalysts or the mixture of commercial Pt/C+RuO_2 (Pt/C:RuO_2 =1:1), where the mass loading of catalyst was about 1 mg cm^{-2}. Nickel foam was used as current collector.

Solid ZABs

2 g of PVA was dissolved in 24 ml of water, the mixture was heated to 95℃ and continuously stirred until it turned into a clear glue-like substance. Then 18 M KOH and 0.6 M $Zn(acac)_2$ aqueous solution was added to obtain a homogeneous solid-state gel electrolyte, and this electrolyte was storaged under -18 ^oC for overnight. Flexible ZABs electrode consists of solid electrolyte, a carbon cloth coated by catalyst as air cathode, and a polished zinc foil as the anode.

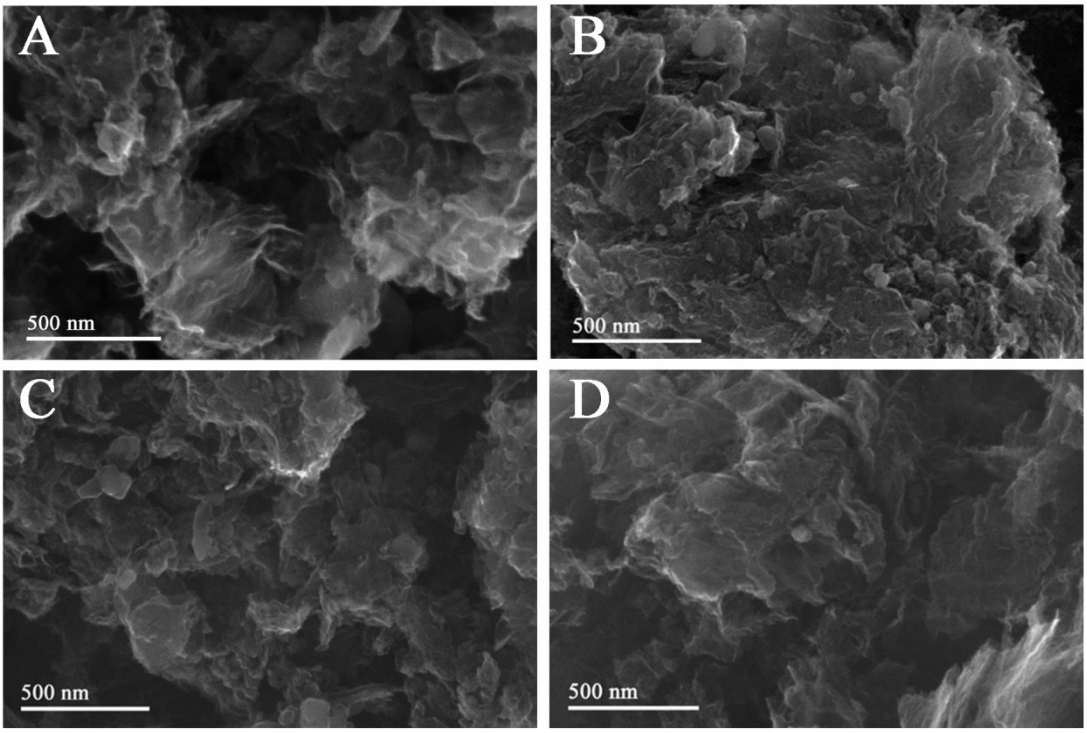

Figure S1 SEM images of (A) NC, (B) Fe-NC, (C) Co-NC and (D) Ni-NC

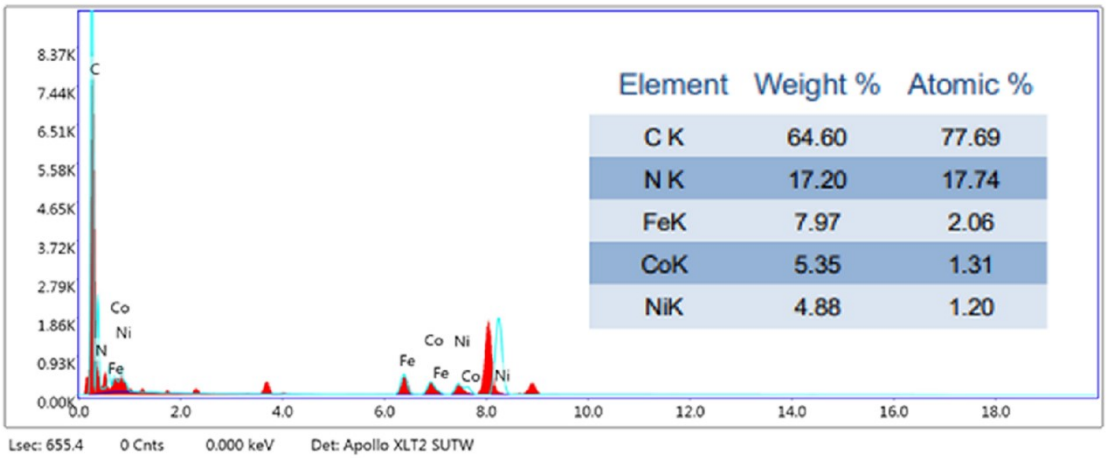

Element	Weight %	Atomic %
C K	64.60	77.69
N K	17.20	17.74
FeK	7.97	2.06
CoK	5.35	1.31
NiK	4.88	1.20

Figure S2 the elemental components of FeCoNi-NC.

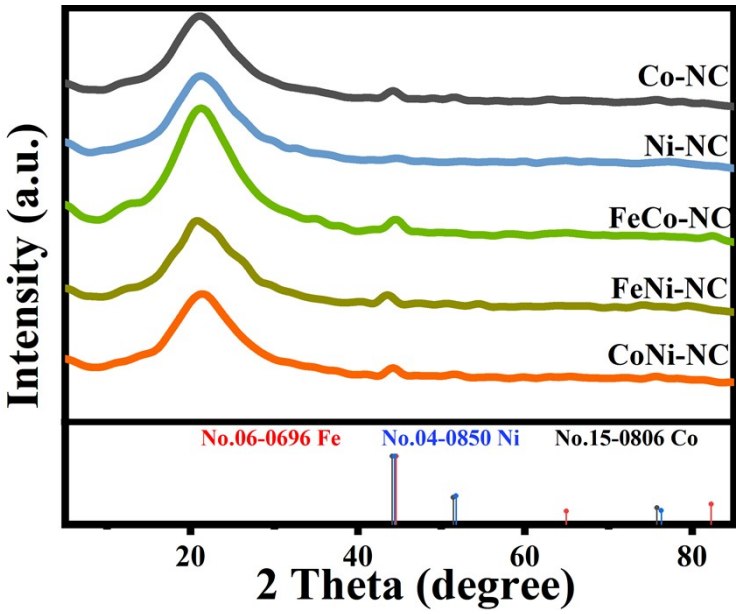

Figure S3 XRD pattern of various samples.

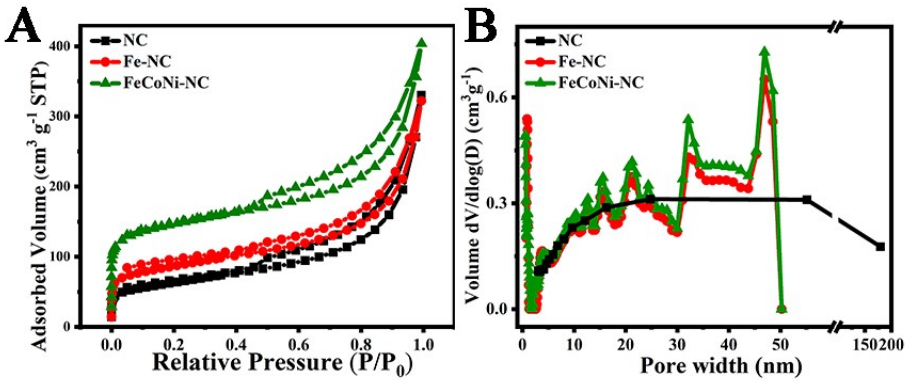

Figure S4 (A) N_2 adsorption-desorption isotherms, and (B) the corresponding pore size distributions of NC, Fe-NC and FeCoNi-NC.

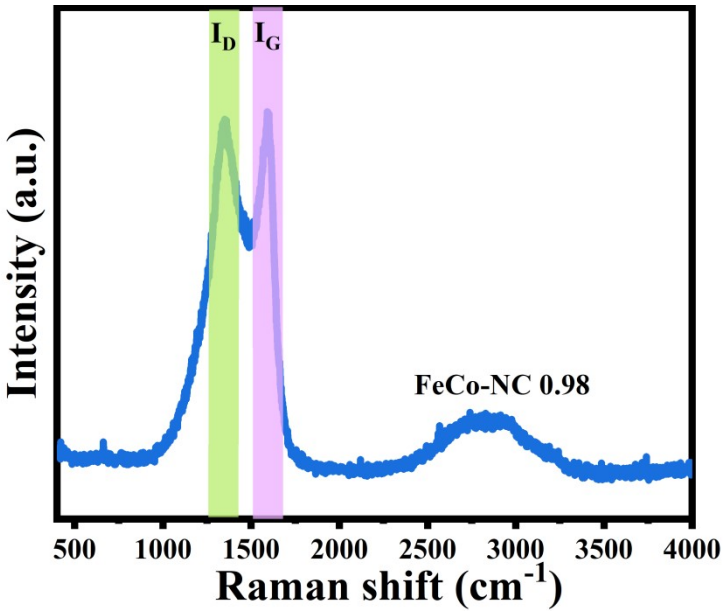

Figure S5 Raman spectrum of FeCo-NC.

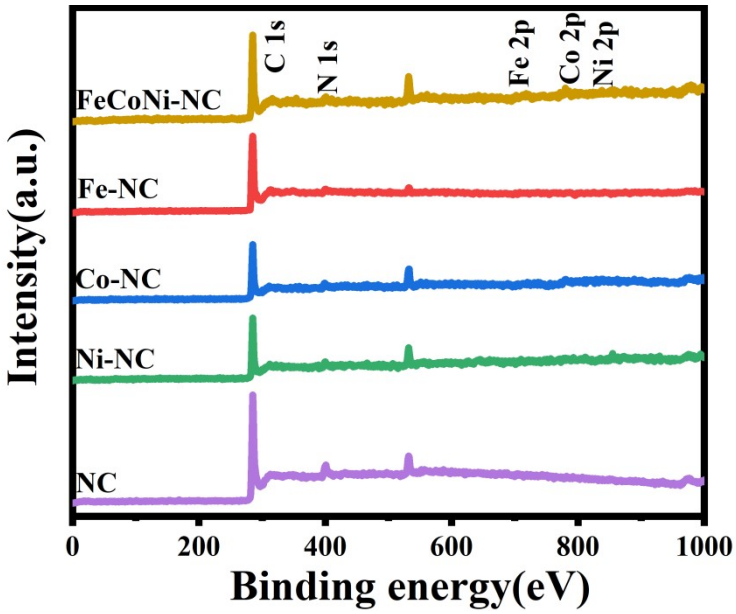

Figure S6 XPS suvery spectra of various samples.

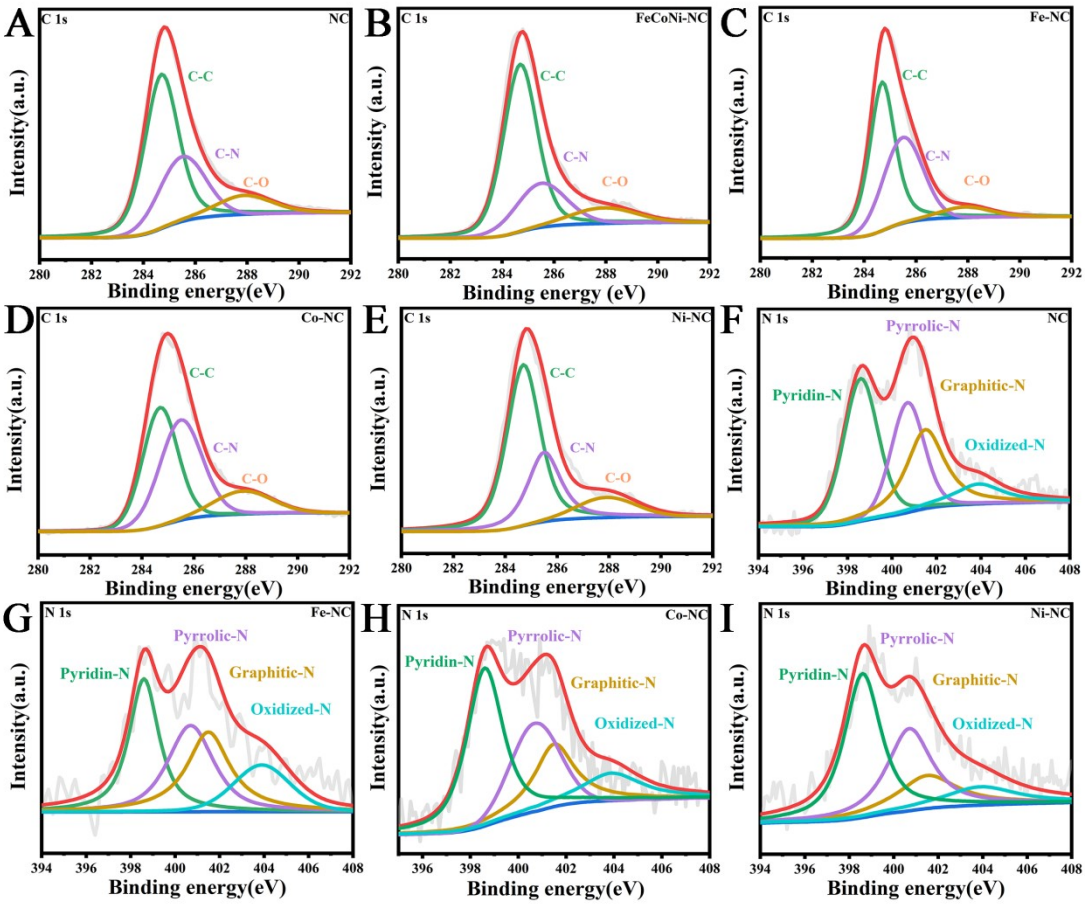

Figure S7 (A-E) C 1s, (F-I) N 1s of various samples.

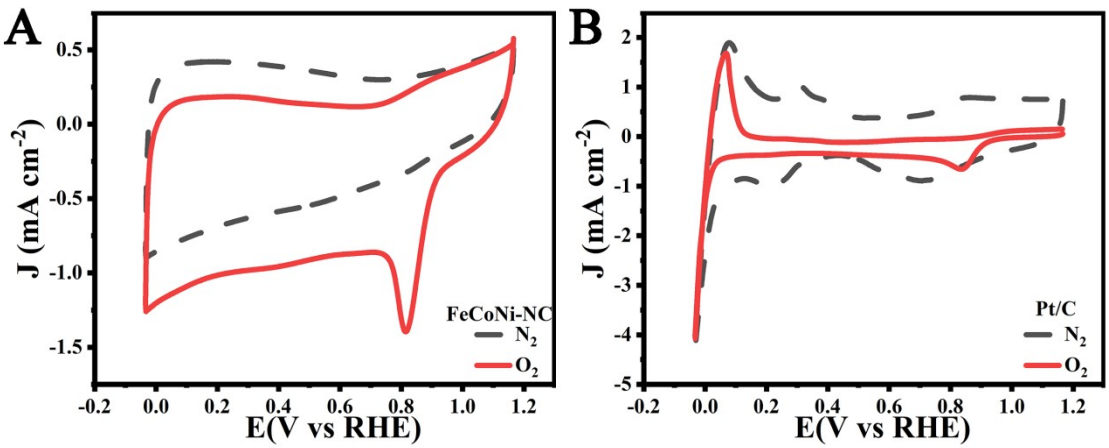

Figure S8 CV curves of FeCoNi-NC and Pt/C in O_2-saturated and N_2-saturated 0.1 M KOH.

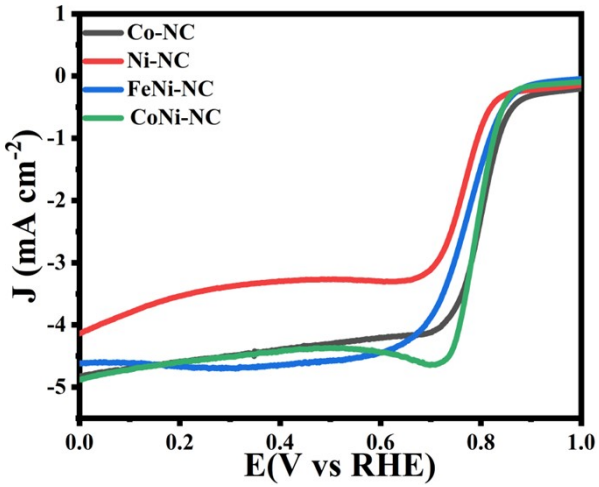

Figure S9 ORR LSV curves of various samples at 1600 rpm in O_2-saturated 0.1 M KOH.

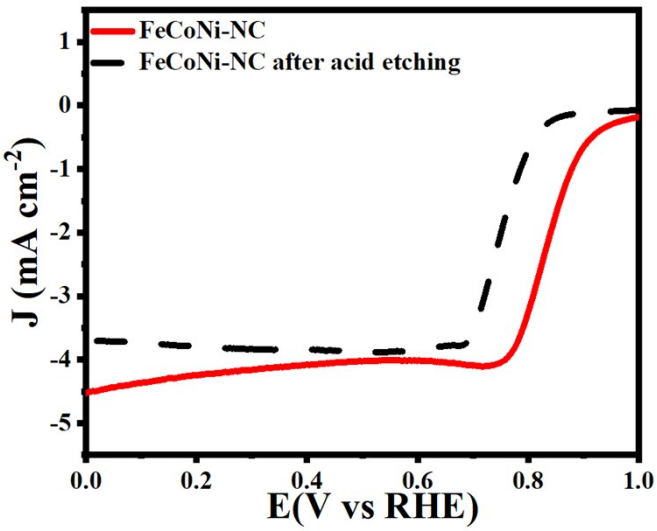

Figure S10 LSV curves of FeCoNi-NC before and after acid etching.

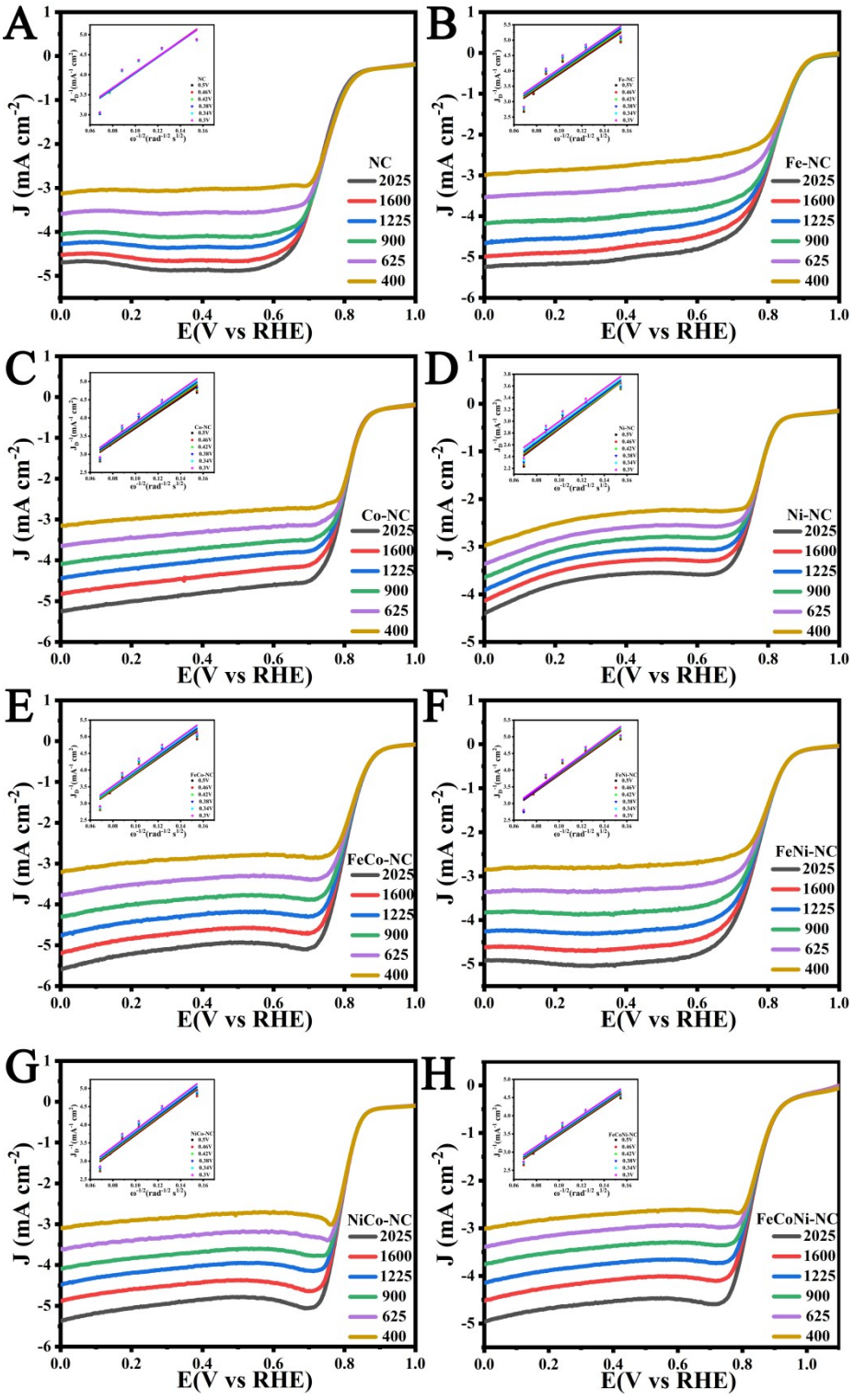

Figure S11 LSV curves with the sweep rate from to 400 to 2025 rpm and the corresponding K-L plots of various samples.

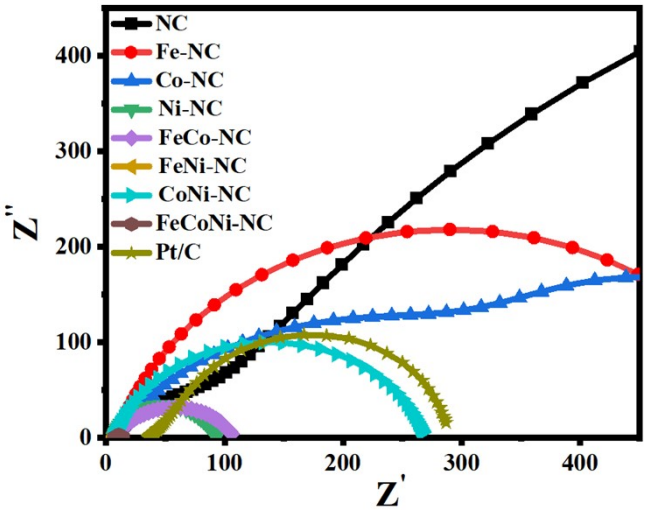

Figure S12 Nyquist plots of various samples in 0.1 M KOH.

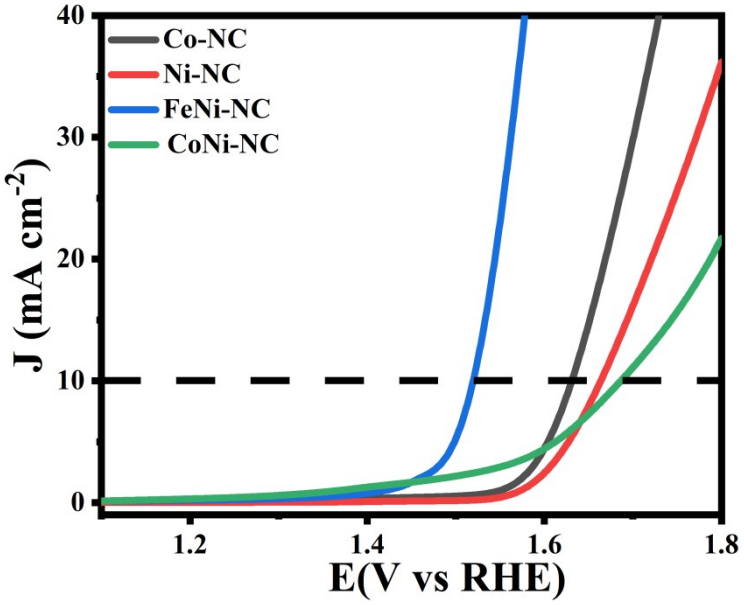

Figure S13 OER LSV curves in 1 M KOH of various samples.

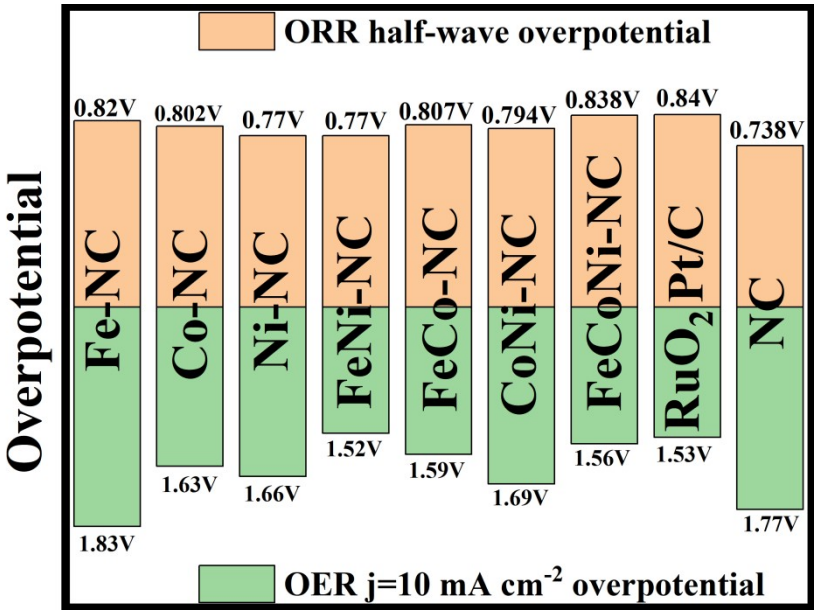

Figure S14 ORR half wave overpotential ($E_{1/2}$) and OER overpotential at 10 mA cm^{-2}.

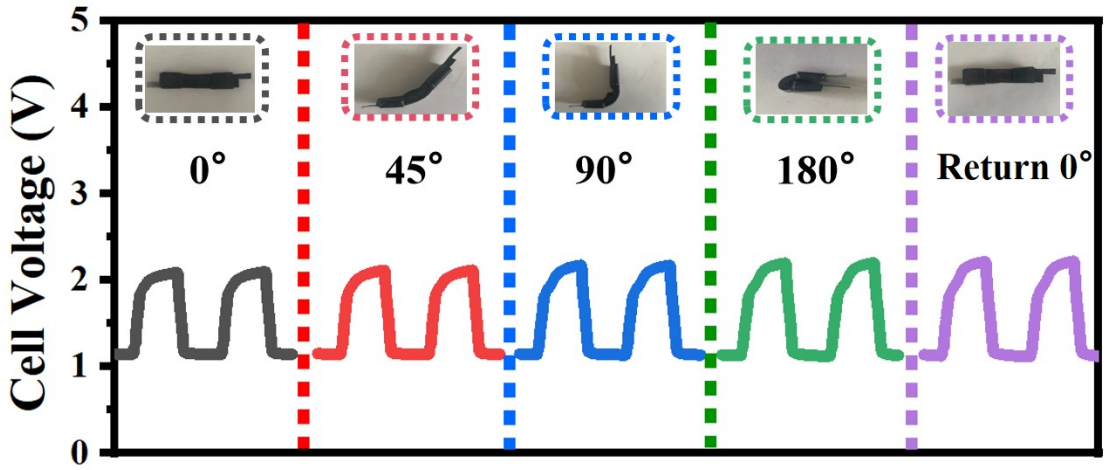

Figure S15 Discharge-charge cycling measurement of FeCoNi-NC-based f-ZABs under bending state (the inset show the images of FeCoNi-NC-based f-ZABs with different bending angles).

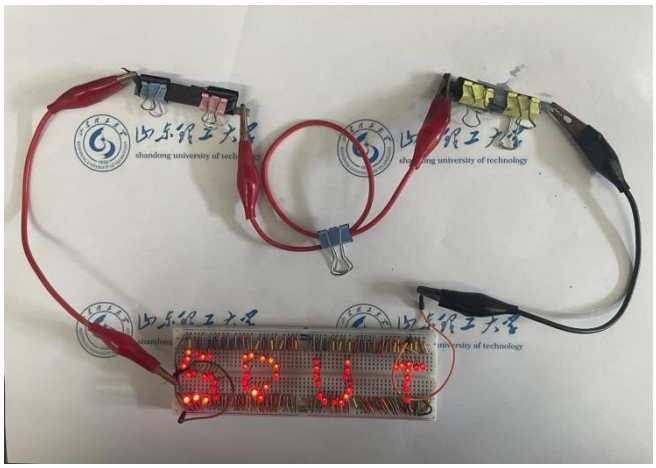

Figure S16 The image of red LEDs powered by FeCoNi-NC-based f-ZABs.

Table S1 Experimental details for as-prepared samples.

Sample	$FeCl_3 \cdot 6H_2O$	$Co(CH_3COO)_2$	$Ni(CH_3COO)_2$
NC	0 mg	0 mg	0 mg
Fe-NC	50 mg	0 mg	0 mg
Co-NC	0 mg	25 mg	0 mg
Ni-NC	0 mg	0 mg	50 mg
FeCo-NC	50 mg	50 mg	0 mg
FeNi-NC	50 mg	0 mg	50 mg
CoNi-NC	0 mg	50 mg	50 mg
FeCoNi-NC	50 mg	25 mg	25 mg

Table S2 The elemental components of as-prepared samples.

Sample	C (at%)	N (at%)	Fe (at%)	Co(at%)	Ni (at%)
FeCoNi-NC	**89.94**	**6.38**	**1.17**	**1.31**	**1.20**
Fe-NC	90.17	8.43	1.41	—	—
Co-NC	90.67	7.00	—	2.33	—
Ni-NC	89.77	8.53	—	—	1.70
NC	91.75	8.25	—	—	—

Table S3 Comparison of ORR and OER activity for FeCoNi-NC with other reported transition metal catalysts.

Sample	ORR $E_{1/2}$ (V)	OER overpotential (V) @ 10 mA cm^{-2}	Reference
FeCoNi-NC	0.838	1.560	This work
FeNi/N-C-800	0.845	1.600	Appl. Catal. B 2023, 321, 122067.
YHP-1	0.79	1.487	Rare Metals 2023. doi.org/10.1007/s12598-023-02485-9.
$Fe_{0.25}Co_{0.75}$/NC-800	0.860	—	Adv. Sci. 2022, 9, 2200394.
NiFe/N-CNT	0.75	1.520	Nano Energy, 2020, 68, 104293.
G-$Co_{0.6}Fe_{0.4}$	0.83	—	Adv. Energy Mater., 2020, 10, 1903215.
FeCo/Co_2P@NPCF	0.79	—	Adv. Energy Mater., 2020, 10, 1903854.
CoFe/N-GCT	0.79	1.670	Angew. Chem. Int. Ed., 2018, 57, 16166-16170.
CoNiFe-S MNs	0.78	1.490	Adv. Energy Mater., 2018, 8, 1801839.